Available online at www.sciencedirect.com
ScienceDirect
Earth and Planetary Science Letters 248 (2006) 772–786
EPSL
www.elsevier.com/locate/epsl

S–Cl–F degassing pattern of water-rich alkali basalt: Modelling and relationship with eruption styles on Mount Etna volcano

Nicolas Spilliaert [a], Nicole Métrich [a,*], Patrick Allard [a,b]

[a] *Laboratoire Pierre Süe, CEA–CNRS, CE-Saclay, 91191 Gif sur Yvette, France*
[b] *Istituto Nazionale di Geofisica e Vulcanologia (INGV), Catania, Italy*

Received 31 January 2006; received in revised form 10 June 2006; accepted 20 June 2006
Available online 24 July 2006
Editor: C.P. Jaupart

Abstract

Our knowledge of the degassing pattern of sulphur, chlorine and fluorine during ascent and eruption of basaltic magmas is still fragmental and mainly limited to water-poor basalts. Here we model and discuss the pressure-related degassing behaviour of S, Cl and F during ascent, differentiation and extrusion of H_2O–CO_2-rich alkali basalt on Mount Etna (Sicily) as a function of eruptive styles. Our modelling is based on published and new melt inclusion data for dissolved volatiles (CO_2, H_2O, S, Cl, F) in quenched explosive products from both central conduit (1989–2001) and lateral dyke (2001 and 2002) eruptions. Pressures are obtained from the dissolved H_2O and CO_2 concentrations, and vapour–melt partition coefficients of S, Cl and F are derived from best fitting of melt inclusion data for each step of magma evolution. This allows us to compute the compositional evolution of the gas phase during either open or closed system degassing and to compare it with the measured composition of emitted gases. We find that sulphur, chlorine and fluorine begin to exsolve at respective pressures of ~140 MPa, ~100 MPa and ≤10 MPa during Etna basalt ascent and are respectively degassed at >95%, 22–55%, and ~15% upon eruption. Pure open system degassing fails to explain gas compositions measured during either lateral dyke or central conduit eruptions. Instead, closed-system ascent and eruption of the volatile-rich basaltic melt well accounts for the time-averaged gas composition measured during 2002-type lateral dyke eruptions (S/Cl molar ratio of 5±1, 35% bulk Cl loss). Extensive magma fragmentation during the most energetic fountaining phases enhances Cl release (55%) and produces a lower S/Cl ratio of 3.7, as actually measured. Comparatively slower magma rise in the central conduits of Etna favours both sulphide saturation of the melt and greater chlorine release (55%), resulting in a distinct S/Cl evolution path and final ratio in eruptive gas. In both eruption types, any previous bubble–melt separation at depth leads to increased S/Cl and S/F ratios in emitted gas. High S/Cl ratios measured during some discrete eruptive events can thus be explained by transitions from closed (deep) to open (shallow) system degassing, with differential gas transfer extending down to ~2 km depth below the vents. This depth coincides with the base of the volcanic pile where structural discontinuities and the high magma vesicularity (60%) may favour separate gas flow. Finally, the excess S–Cl–F gas discharge through Etna summit craters during non-eruptive periods requires a mixed supply from shallow magma degassing in the volcanic conduits and deeper-derived SO_2-rich bubbles from the sub-volcano plumbing system. Our modelling provides a useful reference framework for interpreting the

* Corresponding author. Tel.: +33 1 69 08 85 11; fax: +33 1 69 08 69 23.
E-mail address: nicole.metrich@cea.fr (N. Métrich).

doi:10.1016/j.epsl.2006.06.031

monitored variations of S, Cl and F in Mount Etna gas emissions as a function of volcanic activity. More broadly, the observations made for S, Cl and F degassing on Etna may apply to other basaltic volcanoes with water-rich magmas, such as in arcs.

Keywords: Mt Etna; volatiles; magma degassing; eruptive mechanisms; modelling

1. Introduction

Sulphur, chlorine and fluorine are three important volatile components of magmas and volcanic gas emissions, besides water and carbon dioxide. In addition to influencing melt properties and phase relations [1], they form acid gas species (SO_2, H_2S, HCl, HF, etc.) and metallic compounds in magmatic fluids that are directly involved in the impact of volcanic eruptions upon the environment and the climate [2], as well as in the genesis of igneous ore deposits (e.g. [3]). Moreover, variations of S/Cl/F chemical ratios in volcanic gases have been recognised as precursory signals of eruptions (e.g. [4,5]). Hence, it is of broad interest to determine the initial abundances of these three elements in magmas and their behaviour during magma degassing processes. This can be done by measuring their dissolved content in melt inclusions entrapped in crystals that form during magma rise and differentiation (e.g. [6]) and, complementarily, by measuring their concentration ratios and mass output in volcanic gas emissions.

Basaltic volcanoes are particularly well suited for such measurements. They erupt primitive magmas that often contain deeply-formed olivine crystals with ubiquitous melt inclusions. They also display a great variety of eruptive regimes (from quiescent lava effusions to lava fountains) and generally remain accessible during eruptions. Paradoxically, however, the abundances of S, Cl and F in basaltic magmas were scarcely measured in a systematic way (e.g. [7–9]) and, even less, with simultaneous determination of water and carbon dioxide, the two main volatile components that allow pressure to be determined (e.g. [10–13]). Consequently, the pressure-related behaviour of S, Cl and F during basalt ascent and degassing still remains poorly constrained. Moreover, most of the available information on S and/or Cl (rarely F) pertain to water-poor basalts from mid-ocean ridges (e.g. [14–16]) and hot spots (e.g. [7,17,18]). In such basalts sulphur and chlorine usually exsolve at low pressure $\leq$10 MPa (e.g. [18–20]) and thus track shallow degassing processes. Instead, they may be expected to exsolve at greater depth and in a more complex way in more hydrous, earlier vapour-saturated basalts, the more so since their diffusion coefficients vary with the amount of dissolved water [21]. However, there exits few data for such hydrous basalts, most of which are erupted in subduction zones (e.g. [22] for a review).

Here we focus on alkali basalts erupted by Mount Etna volcano (Italy) which are particularly rich in water ($\geq$3.5 wt.% [11–13]) but also in carbon dioxide ($\geq$1.5 wt.% [23]). We present the first pressure-related model for the degassing of S, Cl and F during ascent, differentiation and eruption of these alkali basalts, using an outmost database for H_2O, CO_2, S, Cl and F dissolved in their olivine-hosted melt inclusions. The data refer to the products of both central conduit and lateral dyke eruptions that occurred in the period 1989–2002 [11–13,24–27], with addition of new results for fluorine in products from the 2002 flank eruption. The evolutions of S, Cl and F in the melt and the gas phase were modelled during either open or closed system degassing, as a function of eruption types. The results allow us to constrain the respective initial exsolution depth of S, Cl and F in Etna magma and to distinguish their different degassing patterns as a function of the dynamics of magma ascent through either the central volcano conduits or lateral dykes that bypass these conduits. Our modelling is then used to discuss and interpret the measured composition of Etna gas emissions during the 2000–2002 eruptive period [28–32] or previously [33,34]. Finally, we examine the potential implications of our conclusions for Etna to other volcanoes erupting water-rich basalts.

2. Volcanological framework

Mount Etna, in eastern Sicily, is a large strato-volcano erupting OIB-type alkali basaltic lavas at near the collision boundary of the African and Eurasian continental plates [35]. Its intense activity includes relatively explosive summit eruptions, ranging in style from Strombolian to fire fountaining and more rarely sub-Plinian, and fissure flank lava effusions that periodically threaten the densely inhabited surroundings [36]. In addition, voluminous gas plume emissions continuously arise from its summit craters [37,38]. This voluminous degassing and the relatively high explosivity of the eruptions are determined by the high volatile richness ($\geq$4 wt.% [11–13,24]) of Etna basaltic magmas, compared to alkali basalts elsewhere.

Since the early seventies, Mount Etna has been increasingly more active [39] and its lavas have evolved spectacularly, becoming more basic, richer in alkalis and radiogenic isotopes (Sr, B), while poorer in chlorine than former lavas (see reviews in [11,40]). It was recently demonstrated that these changes were due to progressive renewal of the plumbing system by a more alkaline volatile-rich basaltic magma with intrinsically higher K_2O/Th, Rb/Th, K_2O/Cl and S/Cl ratios than all previously erupted magmas [11,12,40]. Over the last three decades this new magma has gradually mixed with and replaced the former resident magmas, triggering a succession of powerful summit and flank eruptions. Its first massive direct extrusion occurred during two highly explosive flank eruptions in July–August 2001 and October 2002–January 2003, following its fast ascent from great depth (~15 km below the vents) and through lateral dykes that bypassed the central volcano conduits (e.g. [41,42]). The melt inclusion data base used in this present work concerns the products of both the 2001 and 2002 flank eruptions [11–13] and those from discrete explosive events and lava fountains that occurred at the summit craters (South East crater and Bocca Nuova) in the period 1989–2001 [24,26,27].

3. Brief description of samples and melt inclusion data

All melt inclusions were analysed in olivine crystals of products from explosive activities (scoriae, lava bombs, lapilli), in which their good preservation were guaranteed by rapid quenching. The chemical compositions of bulk rocks and melt inclusions are given in the corresponding publications [11–13,24,26,27]. Note that

Table 1
Dissolved volatiles in melt inclusions from the 2002 samples

Sample	Fo[a]	K_2O	CO_2	H_2O	S	Cl	F	S/Cl	Cl/F	P[b] (MPa)
27–29 October 2002										
7-5c	81.7	1.96	0.236	2.67	0.312	0.163	0.099	1.91	1.65	327
5-41a	81.5	1.94	0.186	3.18	0.295	0.160	0.082	1.85	1.95	310
7-6	82.1	1.99	0.125	2.93	0.313	0.160	0.099	1.96	1.61	234
8-3b	81.3	2.06	0.124	2.84	0.322	0.144	0.080	2.23	1.81	227
8-15a	82.0	1.98	0.078	3.26	0.294	0.153	0.088	1.92	1.75	205
8-4	80.7	1.89	0.063	3.07	0.287	0.144	0.076	1.99	1.89	175
5-26b	78.5	2.82	0.029	1.24	0.182	0.200	0.129	0.91	1.55	55
5-26a	78.5	3.07	0.029	1.10	0.133	0.219	0.147	0.61	1.49	52
11 November 2002										
15-1a	81.1	1.99	0.110	2.56	0.319	0.159	0.098	2.01	1.63	196
15-1e	81.1	2.04	0.117	2.22	0.325	0.168	0.111	1.94	1.51	185
15-6a	80.9	1.96	0.097	2.65	0.338	0.167	0.079	2.02	2.13	187
21 November 2002										
24-1	80.6	2.08	0.176	2.72	0.347	0.174	0.089	2.00	1.95	273
24-7b	81.6	1.98	0.114	2.74	0.318	0.165	0.081	1.93	2.04	211
24-28b	81.3	1.86	0.134	2.37	0.308	0.135	nd	2.27	nd	211
24-41	81.1	2.07	0.112	2.37	0.324	0.157	0.081	2.07	1.93	188
24-28a	81.3	2.01	0.106	2.28	0.315	0.160	0.092	1.97	1.74	177
24-3a	79.1	1.86	nd	2.03	0.291	0.171	0.098	1.70	1.74	nd
09 December 2002										
35-30a	81.7	1.72	0.314	3.19	0.289	0.154	0.074	1.87	2.08	426
35-30b	81.7	1.77	0.147	3.06	0.294	0.160	0.077	1.83	2.07	265
35-16	80.0	2.00	0.114	2.82	0.314	0.162	0.082	1.93	1.99	216
35-10	81.3	2.19	0.103	2.82	0.330	0.159	0.092	2.08	1.74	203
35-6	80.0	1.86	0.113	2.44	0.299	0.161	0.096	1.86	1.67	193
35-9	81.7	2.03	0.086	2.20	0.308	0.155	0.089	1.98	1.75	152
35-1	81.5	1.99	0.052	2.72	0.314	0.162	0.096	1.94	1.68	141
35-31a	74.8	2.95	0.015	0.34	0.048	0.213	0.131	0.23	1.63	24
35-31b	74.8	2.72	nd	0.67	0.099	0.188	0.115	0.53	1.63	nd

The melt inclusion compositions are corrected for post-entrapment olivine crystallisation (≤5%, [12]). nd: not determined.

[a] Host olivine composition (Fo in mol% = 100 × [Mg/(Mg+Fe)]).

[b] Total fluid pressures computed from dissolved H_2O and CO_2 using Volatilecalc program [49] are published in Spilliaert et al. [12].

lavas commonly erupted from Etna central conduits (~summit eruptions) are plagioclase-dominated trachybasalts (e.g. [43]), whereas the 2001 and 2002 flank eruptions produced plagioclase-free basalts to trachybasalts [12,32,40,43]. Melt inclusion data for pre-2000 products were selected on basis of K_2O/Cl and S/Cl ratios, in order to play with a coherent data set representative of the new magma and to minimize the effects of magma mixing on dissolved K_2O, S, Cl and F contents. We summarise below the most relevant features of the samples.

We also report here new results for fluorine in the 2002 samples (Table 1). These were obtained with a CAMECA IMS6f ion microprobe at the CIG (Ecole des Mines, Fontainebleau, France), using a Cs^+ primary beam, 5–10 μm analysed zone size and ^{18}O as internal standard. Fluorine contents were calibrated against the following reference glasses: NBS612 (55±2 ppm), ALV981R23 (±3 ppm), VNM (1010±20 ppm), CFA47 (2270±20 ppm) and KE12 (3830±90 ppm) [44,45].

3.1. Primitive olivines and their entrapped melts

Magnesium-rich olivine microphenocrysts ($Fo_{82.5–79.0}$) predominate in the 2001 and 2002 basaltic–trachybasaltic products, as well as in those from most energetic lava fountains that occurred at the Southeast summit crater in April 2000 [13] and February 1999 [26,27]. Melt inclusions in these olivines are chemically similar to the host basalts–trachybasalts (Fig. 1a) and represent the primitive stage of differentiation of present-day Etna magma (MgO up to 7.2 wt.%, $K_2O \leq 2$ wt.%; Fig. 1a–b). They contain 3.6 to 2.1 wt.% H_2O and from 0.41 to 0.05 wt.% CO_2. Their concentrations in sulphur (0.27 to 0.35 wt.%), chlorine (0.13 to 0.18 wt.%) and fluorine (0.08 to 0.11 wt.%) tend to increase along with melt evolution, while S/Cl (2), Cl/K_2O (0.081) and F/K_2O (0.045) ratios remain constant. This population of primitive inclusions is never saturated with an immiscible sulphide.

In addition, the olivine microphenocrysts often contain more evolved ($K_2O > 2.5$ wt.%; Fig. 1a–b) glass embayments – glass pockets either isolated in the crystal or connected with the surrounding matrix – that occasionally reach the matrix glass composition. These embayments are poorer in H_2O (1.3–0.3 wt.%) and S (0.22–0.01 wt.%) but richer in Cl and F (up to 0.26 and 0.17 wt.%, respectively) than the melt inclusions.

3.2. Fe-rich olivines and their melt inclusions

Less magnesian olivines ($Fo_{72–69}$) commonly prevail in trachybasaltic lavas and tephra erupted from the summit craters. Their melt inclusions are usually evolved ($K_2O > 2.4$ wt.%; Fig. 1a–b) and depleted in H_2O (<1.5 wt.%), CO_2 (<0.05 wt.%) and S (from ~0.13 to ≤0.03 wt.%). Their Cl content ranges from 0.25 to 0.15 wt.%. Moreover, they often contain a Fe–Cu-rich sulphide globule, associated with Fe–Ti oxide, which shows that the magma was saturated with an immiscible sulphide. This latter is systematically observed in melt inclusions of Fe-richest olivines [24,46,47] and as solid inclusions in clinopyroxene [48] of the trachybasalts. This population of inclusions is representative of partially degassed, plagioclase-bearing magma that has been stored at quite shallow levels in the central volcano conduits.

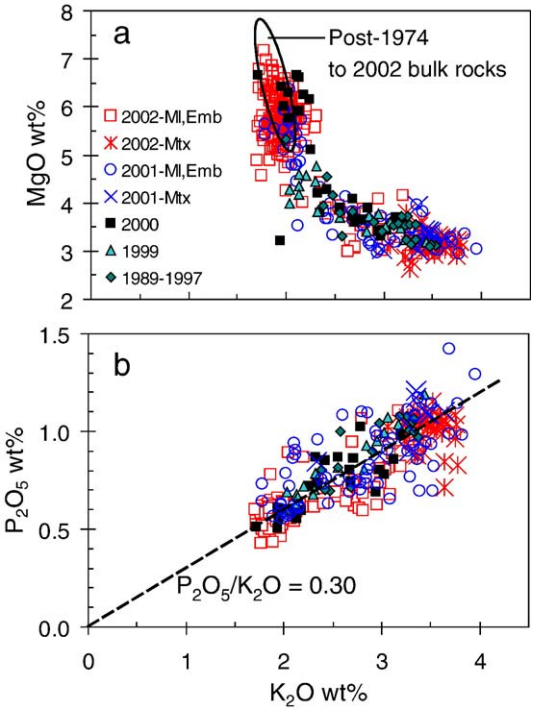

Fig. 1. Evolution of MgO (a) and P_2O_5 (b) vs. K_2O in olivine-hosted melt inclusions, embayments and matrix glasses of products from lateral dyke and central conduit eruptions of Etna. Lateral dyke eruptions: 2001 lower vents (LV, 2500–2100 m a.s.l.) and 2002 south vents (SV) [11,12]. Central conduit-related eruptions: Strombolian activity at 2001 upper eruptive vents (UV, 2700 m a.s.l; [11]); Southeast summit crater (SEC): April–June 2000 [13] and February 1999 [26,27] lava fountains; October 1989 and August 1990 explosive eruptions [24]; Bocca Nuova crater: 1997 Strombolian activity [27].

3.3. Matrix glasses

Matrix glasses represent the ultimate stage of the magma differentiation trend ($K_2O = 3.5 \pm 0.2$ wt.% on average; Fig. 1a–b). Their low residual concentrations of H_2O (≤0.2 wt.%), CO_2 (<0.005 wt.%) and S (<0.02 wt.%)

indicate a bulk loss of ≥95% for these three main volatile species upon magma ascent and extrusion in either eruption type. Instead, chlorine is more variably and less depleted. Matrix glasses in plagioclase-poor products of the 2001 and 2002 flank eruptions contain between 0.27 and 0.17 wt.% Cl, implying from 0% to ~40% Cl loss. The latter value matches the estimate of 35% deduced from the whole rocks ($Cl/K_2O = 0.053 \pm 0.002$). In comparison, matrix glasses in trachybasaltic samples from the summit craters contain 0.16 to 0.13 wt.% Cl, evidencing a more extensive release of chlorine (up to 55%) that is also verified in the bulk rocks ($Cl/K_2O = 0.036 \pm 0.004$). Finally, using the measured F content of the 2001 and 2002 bulk rocks ($F/K_2O = 0.035 \pm 0.004$), corrected for crystallisation, we estimate a maximum loss of 15% for fluorine during lateral dyke eruptions.

4. Pressure-related modelling of S, Cl and F degassing

4.1. Basic considerations

The dissolved concentrations of sulphur, chlorine and fluorine in melt inclusions allow us to model the magma degassing pattern during decompression and differentiation. The constant P_2O_5/K_2O ratio during magma evolution (Fig. 1b) excludes any measurable fractionation of Cl and F by crystallising apatite, an uncommon mineral phase in Etna lavas. In contrast, sulphide immiscibility during shallow crystallisation in the central conduits should influence the degassing path of sulphur. The low residual S content (≤0.01 wt.%) of all bulk rocks and their lack of sulphide globules, however, imply a minor, temporary and perhaps very local influence of sulphide saturation on the bulk sulphur budget [47].

We have modelled the behaviour of S, Cl and F during Etna magma ascent, differentiation and eruption under both open and closed system conditions.

1. During open system degassing (OSD), the exsolved vapour phase continuously escapes from the melt and the dissolved concentration of a given volatile species, *Xi*, follows a Rayleigh distillation law:

$$X_i = X_{i0} \times f^{D_i - 1} \quad (1)$$

where X_{i0} is the initial concentration of species (i), D_i its vapour–melt bulk partition coefficient and f the fraction of melt after each step of crystallisation. f is given by the $(K_2O)_0/(K_2O)$ ratio, where $(K_2O)_0$ is the initial K_2O content of the primitive melt (1.75 wt.%). Plotting $\ln(X_i)$ vs. $\ln(K_2O)$ produces linear trends with slope $(1-D_i)$, which thus enable one to directly assess D_i values and their evolution with magma differentiation.

2. During closed system degassing (CSD), the gas phase continuously re-equilibrates with the melt and the concentration of species (i) is given by the mass balance equation:

$$X_i = X_{i0}/[D_i + (1-\alpha_0)f] \quad (2)$$

While X_i and f are as defined in Eq. (1), X_{i0} here is the initial amount of species (i) in the total system (melt+vapour), D_i is its vapour–melt bulk distribution coefficient, and α_0 is the mass fraction of CO_2–H_2O vapour that may already exist at the depth of initial exsolution of species (i). $D_i = \alpha D_I^*$, where D_I^* is the instantaneous gas–melt partition coefficient and α the mass fraction of total vapour that is accumulated at each step of degassing upon ascent:

$$\alpha = \alpha_{0+}[(X_{oH_2O_{melt}}/f) - X_{H_2O_{melt}}] \quad (3)$$

(X_{H_2Omelt}) is the dissolved H_2O concentration of the melt at differentiation stage f, constrained by the covariation of H_2O with K_2O in melt inclusions. At 400 MPa, X_{oH_2Omelt} in Etna basalt averages 3.4± 0.2 wt.%, while X_{CO_2} is only 0.3 wt.% [11,12]. Given the estimated original CO_2 content of ~1.5 wt.% in Etna parental magma [23], at that pressure the basaltic melt should already coexist with an exsolved gas phase composed of 1.2 wt.% CO_2+0.3 wt.% H_2O [12]. We thus considered $\alpha_0 \sim 0.015$. During further decompression up to the surface, the evolution of α is prevalently determined by H_2O exsolution.

The total fluid pressure at saturation for each inclusion analysed for S, Cl and F was inferred from the co-dissolved concentrations of CO_2 and H_2O and from the VOLATILECALC software [49]. Details of the calculations and their limitations are discussed in [11,12]. Fig. 2 shows the pressure-calibrated evolution of S/Cl ratio in melt inclusions, glass embayments and matrix glasses. The corresponding lithostatic depths of melt entrapment (or degassing) were derived from the density of lithologies in Etna crustal basement [50] and are subsequently reported as depths below eruptive vents (except when specified). This allows us to determine the depth-related variations of S–Cl–F in the melt and then in the gas phase. The evolution of S/Cl/F ratios in the gas phase was modelled from the computed D_i values and the following relationship:

$$(X_i/X_j)_{gas} = (D_i/D_j) \times (X_i/X_j)_{melt} \quad (4)$$

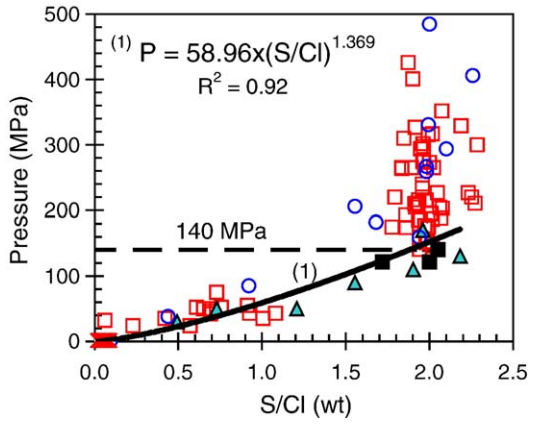

Fig. 2. Pressure-related evolution of S/Cl ratio in melt inclusions, glass embayments and matrix glasses. Data from 2001 and 2002 lateral eruptions [11,12] and SEC lava fountains (16 April 2000 [13]; 4 February 1999 [27]). Symbols as in Fig. 1. P=total fluid ($P_{CO_2}+P_{H_2O}$) pressure calculated from the co-dissolved contents of CO_2 and H_2O and the Volatilecalc solubility model [49]. The evolution of S/Cl ratio is calibrated between ≤140 MPa and the surface, as no sulphur exsolution occurs prior to ~140 MPa (constant S/Cl ratio ~2; see text).

4.2. S–Cl–F evolution in melt

Fig. 3 displays the ln–ln evolutions of S, Cl and F vs. K_2O in the ascending and differentiating melts involved in lateral dyke and central conduit eruptions of Etna, as constrained by melt inclusion data. Best fitting of the data provides us with the vapour–melt partition coefficients during either open or closed system degassing. The respective bearing of each process is subsequently discriminated from modelling of the gas phase (Figs. 4 and 5).

4.2.1. Lateral dyke eruptions

Melt inclusions from the 2001 and 2002 flank eruptions show a well-defined sulphur behaviour during melt decompression and evolution (Fig. 3a). A pure OSD process would involve three degassing stages, marked by two abrupt slope changes at f values of 0.83 (~140 MPa) and 0.53 (10 MPa). During the first stage, sulphur increases in the melt and is little exsolved (D_S=0.35±0.1). Instead, the second stage (D_S=4.6) corresponds to massive sulphur partitioning into the gas phase, reducing the melt content from 0.32 to ~0.06 wt.%. The third stage (D_S=25) characterises very shallow degassing and leads to residual S concentrations at the detection limit (~0.008 wt.%). In a CSD process, the overall evolution of dissolved sulphur is fitted with $D_S=\alpha D_S^*$ values that increase from 0 to 60.

Chlorine exhibits a less defined behaviour (Fig. 3b). Within the error limits, the melt preserves a constant Cl/K_2O ratio (0.081±0.005) until f=0.74 or P~100 MPa, implying no Cl exsolution before that depth. Subsequently, the behaviour of chlorine strongly depends on the dynamics of magma ascent and extrusion (Section 4.3). A large proportion of evolved inclusions and matrix glasses points to a low bulk Cl loss of 22% (Cl/K_2O=0.065), implying D_{Cl}=0.5 in case of OSD and D_{Cl} from 0 to 0.13 in CSD. Other samples however show a greater chlorine loss, averaging 35% (Cl/K_2O=0.053). This latter trend can be accounted for by either a two-stage OSD process with D_{Cl}=0.5 until f=0.53 (10 MPa) and D_{Cl}=3.6 between 10 MPa and the surface, or a CSD process with D_{Cl} gradually varying from 0 to 0.32.

Fluorine starts to outgas at much lower pressure than both sulphur and chlorine, the F/K_2O ratio (0.045) of the melt remaining constant until ~10 MPa (f~0.53; Fig. 3c). Fluorine degassing between 10 MPa and the surface cannot be modelled owing to the lack of data for matrix glasses. However, using the F content and F/K_2O ratio (0.035) of bulk erupted scoriae, the inferred 15% loss of fluorine during late stage magma degassing suggests D_F~2.6 in OSD or D_F varying from 0 to 0.12 in CSD.

4.2.2. Central conduit eruptions

Compared to lateral dyke eruptions, magmas erupted across the central conduits of Etna show quite a distinct behaviour of S and Cl (Fig. 3d–e).

Sulphur concentrations define two distinct trends corresponding to magmas that were saturated or not with respect to sulphide globules (Fig. 3d). The most primitive melt inclusions from powerful lava fountains at SEC (4 February 1999 and 16 April 2000) were never saturated in sulphide and display a sulphur degassing pattern very similar to that of primitive melt inclusions from lateral dyke eruptions. We thus infer similar conditions of magma ascent, differentiation and degassing (*i.e.*, similar D_S values in either closed or open system).

The melt inclusions containing a sulphide globule and/or representative of sulphide-saturated magma plot in a distinct domain at a given K_2O value (f=0.76–0.58 and S=0.13–0.04 wt.%; Fig. 3d). In this domain their evolution under OSD conditions can only be modelled with a D_S of 4.6, that increases to 11 when sulphide globules disappear during late stage melt degassing (f<0.58). However, a CSD process starting from ~140 MPa (f=0.83) and with varying bulk D_S best fits the entire data set. In this case, $D_S=\alpha D_S^{vap/melt}$ when the magma is sulphide under-saturated and $D_S=\alpha D_S^{vap/melt}+\beta D_S^{FeS/melt}$ in the domain of sulphide saturation. Heating experiments performed on analogous water-rich basaltic melt inclusions from nearby Stromboli volcano showed that ~52% of total

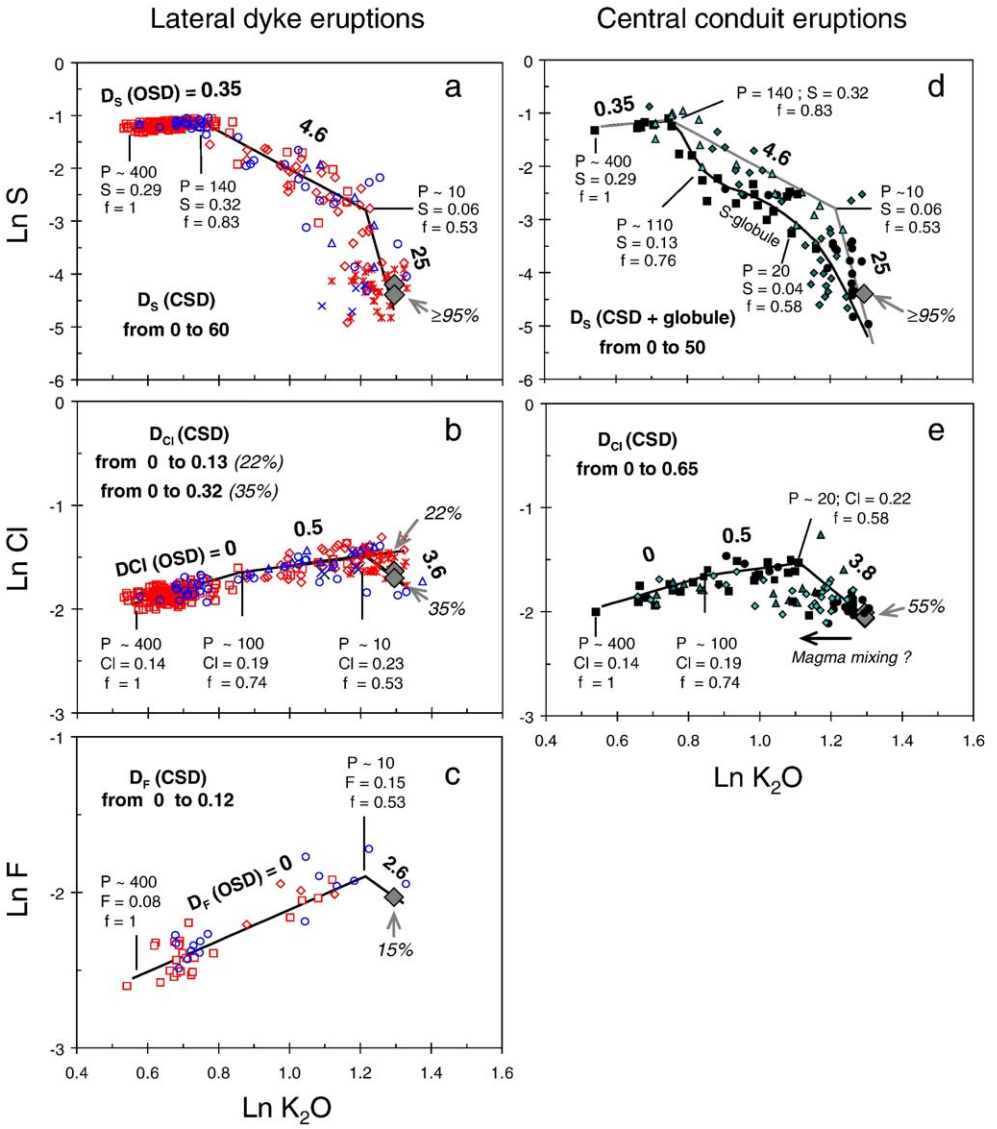

Fig. 3. ln–ln variations of dissolved sulphur, chlorine and fluorine during melt evolution (K_2O) and decompression in case of lateral dyke (a–c) and central conduit (d–e) eruptions. Symbols in a–c are: 2002 (SV) samples: MI (square), embayment (lozenge), matrix (asterisk); 2001 (LV) samples: MI (circle), embayment (triangle), matrix (cross). Symbols in Fig. 3 d–e are: samples of 2001 UV (circle); 2000 (square); 1999 (triangle); 1989–1990 and 1997 (lozenge). In each plot, we indicate the total pressure (MPa), the fraction of remaining melt ($f=K_2O_0/K_2O$) and the S or Cl or F concentration (wt.%) at major steps of evolution. Best data fitting provides the vapour–melt partition coefficients D_S, D_{Cl} and D_F during either open system degassing (OSD) or closed system degassing (CSD). Note the difference in scale for LnS, LnCl and LnF. Concentrations in bulk matrix glasses (grey lozenges) refer to the residual volatile concentrations measured in bulk rocks and normalised on basis of the final K_2O content (mean: 3.65 wt.%). The corresponding bulk percentages of S, Cl and F loss are indicated in italic. Panel d shows the distinct data points for sulphide-saturated magma. See text for discussion.

dissolved sulphur can be removed by the sulphide globule, which corresponds to $D_S^{FeS/melt}=475$ [51]. Therefore, we used this value and the $\alpha D^{vap/melt}$ range (0 to 50) determined for a CSD evolution of primitive inclusions to draw the corresponding curve in Fig. 3d.

Like in lateral dykes, no chlorine exsolves in the central conduits before ~100 MPa ($f=0.74$; Fig. 3e). Afterwards, the evolution of chlorine may follow a two-stage OSD process with $D_{Cl}=0.5$ and 3.8, respectively, marked by an abrupt change at 20 MPa ($f=0.58$). The same data can be fitted by a CSD process in which D_{Cl} would vary from 0 to 0.65. The most important difference relative to lateral dyke eruptions is that chlorine degasses more extensively during central conduit eruptions (55%, $Cl/K_2O=0.036$; Fig. 3e). The relative scattering of pre-2000 degassed samples, compared to post-2000 ones,

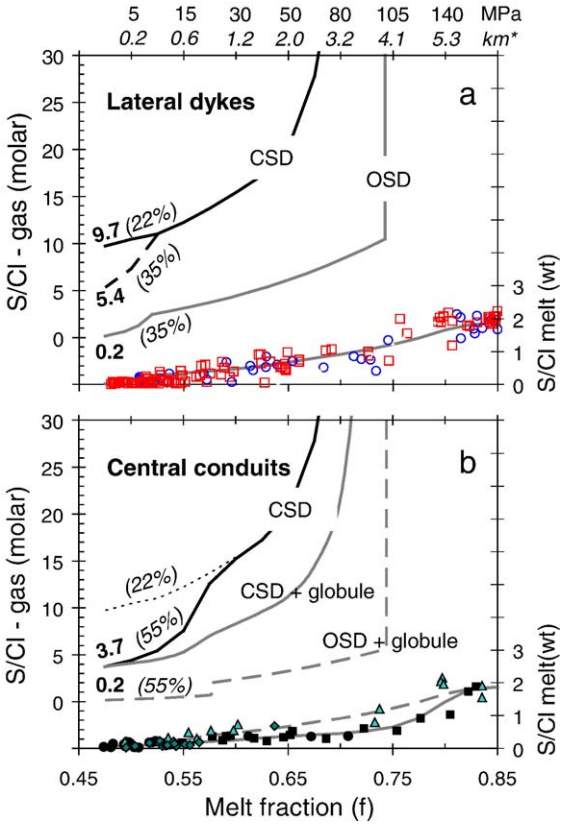

Fig. 4. Pressure-related variations of S/Cl ratio in the melt and the gas phase under open and closed system conditions during lateral dyke (a) and central conduit (b) eruptions of Etna. The melt ratios (right-hand axis) are kept in weight, while the modelled gas ratios (left-hand axis) are given in mole in order to facilitate their subsequent comparison with values measured in Etna gas emissions. Lithostatic depths below vents (*km**) are computed from pressure values (MPa) and rock densities in the sedimentary basement of Etna [50]. CSD curves and the final bulk ratio in surface gas take account of the differences in mean bulk Cl loss (from 22% to 55%) observed in respective residual glasses. Pure OSD conditions produce much lower S/Cl ratio (<0.2) in surface gases than measured in emissions of both eruption types (see text). CSD and OSD curves in panel (b) illustrate the significant influence of sulphide immiscibility on S/Cl degassing path in the central volcano conduits.

suggests the additional influence of possible mixing between magmas that differed in either their degree of differentiation (and Cl content) or their initial K_2O content (variable imprint of the former K-poorer resident magmas; e.g. [11]).

4.3. S/Cl/F variations in the magmatic gas phase

Figs. 4 and 5 show the computed evolutions of S/Cl, S/F and Cl/F ratios in the magmatic gas phase as functions of pressure and melt differentiation in lateral dykes and/or central conduits, under either open or closed system conditions. OSD and CSD processes lead to markedly different evolutions of the gas phase and contrasting final ratios in eruptive gas emissions.

4.3.1. S/Cl ratio

Because no chlorine exsolves prior to 100 MPa, as shown above, our results for S/Cl ratio (Fig. 4a–b) apply to magma degassing between that pressure and the surface. Moreover, the S/Cl ratio of the gas phase is principally controlled by sulphur outgassing until about 10–20 MPa and becomes influenced by chlorine exsolution only at lower pressure, as the melt is already severely depleted in sulphur.

In both lateral dyke and central conduit eruptions, a pure OSD process starting from 100 MPa would produce a very sharp drop of S/Cl ratio in the exsolving gas, from an initial value of ~30 down to very low values ≤0.2 at the surface for a Cl loss varying from 35% to 55%. Now, such low final values are very uncommon in vent degassing on Etna [28,34] and, rather, characterise the residual degassing of lava flows [29,52]. Instead, in a CSD process the S/Cl ratio of the gas phase evolves more progressively, from an initial value ≫30 at 100 MPa to a bulk surface value that differs between lateral dyke and central conduit eruptions. In a lateral dyke, S/Cl drops to ~12 at 15 MPa (Fig. 4a) and ranges between ~9.7 and

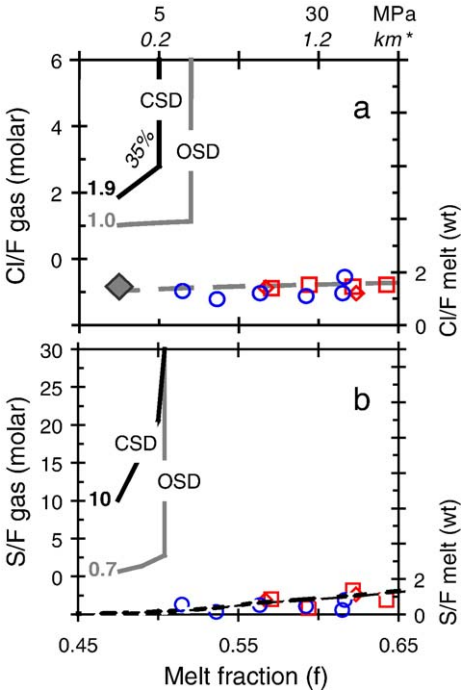

Fig. 5. Pressure-related variations of Cl/F (a) and S/F (b) ratios in the melt and the gas phase under open and closed system conditions during 2002-like lateral dyke eruption.

5.4 at the surface for a chlorine loss of 22% to 35%, as observed in 2001 and 2002 eruptive products. In comparison, at 15 MPa the gas phase produced by CSD in the central conduits has a S/Cl ratio of ~5 or 7, depending on whether the magma is saturated or not with sulphide (Fig. 4b). In either case, however, the surface gas has a bulk S/Cl ratio of ~3.7, significantly lower than computed for lateral dyke eruptions.

Thus, the evolution path and final composition of the magmatic gas phase in terms of S/Cl ratio depend on the dynamics of ascent, differentiation and degassing of the magma in either lateral dykes or central conduits. Pure OSD and CSD processes represent two limiting cases, since intermediate conditions or transitions between these two processes may occur and lead to more complex S/Cl evolutions. As a general rule, any pre-eruptive differential ascent of gas bubbles (opening system) from a magma initially rising as a closed system will give rise to higher S/Cl ratio in surface gas emissions, depending on the depth and extent of bubble–melt separation.

4.3.2. Cl/F ratio

Given the very shallow initial exsolution of fluorine (~10 MPa), theoretical modelling of Cl/F and S/F ratios is possible for only late degassing and evolution of the magma (Fig. 5). Closed system degassing in lateral dykes generates a bulk gas phase with final Cl/F and S/F ratios of ~1.9 and 10, respectively, for a mean Cl loss of 35%. Under pure OSD conditions, the corresponding values would be ~1 and ~0.7. Despite limited constraints on F in residual melts, the S/F ratio of magmatic gas emissions could thus be a sensitive marker of either open or closed system degassing conditions at shallow level.

5. Discussion

5.1. S, Cl and F degassing behaviour at Etna and other basaltic volcanoes

5.1.1. Sulphur

Sulphur solubility in basalts strongly depends on redox conditions and thus the relative proportions of sulphate and sulphide dissolved in the melt (e.g. [1,53,54]). In primitive Etna melt inclusions the proportion of total sulphur dissolved as sulphate was estimated to be ~60% by using electron microprobe [27,55], but more accurate measurements using X-ray absorption micro-spectroscopy [56] indicate a proportion closer to 80% [Metrich et al., unpublished]. Such a large predominance of sulphate in Etna alkali basalts is consistent with their high water content and oxidised state [27,55], and helps explain their high sulphur content.

Sulphide immiscibility never occurs during the initial stage of basalt ascent and differentiation (Section 3.1) and no or little sulphur is exsolved prior to a pressure of ~140 MPa, *i.e.* before the magma reaches about 5.5 km depth below the vents (Section 4.2.1). Simple sulphur outgassing by decompression at that level is compatible with thermodynamic modelling for water-rich basalt [53]. However, this pressure also marks a transition from which sulphur outgassing can become affected by sulphide immiscibility in magma slowly rising towards the summit craters. This is well seen in Fig. 6 from the decoupled evolution of dissolved sulphur and water: for a same H_2O content of ~1.5 wt.% ($P \sim 50$–30 MPa) sulphide-saturated melt trapped as inclusions in olivine Fo<75 (central conduits) contains twice less sulphur than sulphide-free melt trapped as glass embayments in olivine Fo ~ 80 (lateral dyke eruptions). Slow magma ascent in central conduits thus favours both sulphide saturation and a more extensive equilibrium crystallisation (including plagioclase and Fe–Ti oxides) of the melt, which in turns affects the sulphur outgassing path. Instead, faster magma ascent inhibits these processes until low pressure, allowing a pure control of sulphur outgassing by vapour–melt partitioning.

5.1.2. Chlorine

Our data demonstrate that chlorine exsolution begins at $P \leq 100$ MPa but remains one order of magnitude lower than that of sulphur until 10 MPa. It becomes important only during shallower magma degassing. There are very little data in the literature for the initial exsolution pressure of chlorine in other basalts. A critical

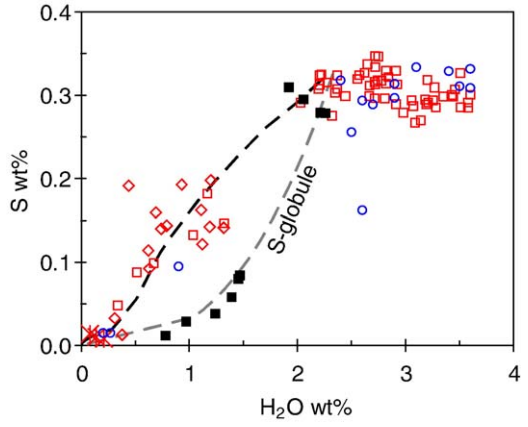

Fig. 6. Respective evolutions of sulphur and water during degassing of melts saturated or not with sulphide. At ~1.5 wt.% H_2O, dissolved sulphur is twice less abundant in sulphide-saturated melt erupted across the central conduits (filled squares, SEC lava fountains in 2000) than in under-saturated melts (open symbols, 2001 (LV) and 2002 (SV) eruptions). Symbols as in Fig. 3.

water depth of 500 m (5 MPa), marked by a strong increase in vesicularity, was indicated for submarine basalts of the Reykjanes Ridge [19]. Otherwise, no appreciable Cl degassing was observed in submarine basalts extruded between 4000 and 400 m water depth at other sites (e.g. [15,18,57]). The high water content of Etna basalt and the high proportion of exsolved gas at 100 MPa (~40%; Fig. 7) may explain why chlorine starts to exsolve at relatively high pressure at Etna. Considering that the Cl/H_2O ratio (~0.05) of Etna basalts is comparable to that of arc magmas (see [22] for a review), one might then expect a comparable behaviour of chlorine in water-rich arc basalts.

The bulk degassing rate of chlorine from Etna magma (from 22% to 55%) is comparable to estimates for Stromboli (40–70% [10]) and the Laki 1783 eruption (40–50% [9]), but is higher than inferred at Kilauea (~10% [58]). As we show here, chlorine degassing strongly depends on the dynamics of magma ascent and extrusion and therefore on kinetic effects. This observation is supported by recent decompression experiments on water-rich rhyolitic melts [59]. These demonstrate that the amount of Cl retained in matrix glass depends on the size of erupted pumice clasts, and that clasts with thinner walls allow more Cl to escape. Similar effects may occur in basalts, in which Cl diffusion would be faster. A higher degree of magma fragmentation should then enhance Cl loss, as shown below.

5.1.3. Fluorine

Experimental studies of fluorine solubility in basalt are missing and natural constraints on F degassing are quite poor. No fluorine loss was detected in most studies of submarine glasses and lavas (see [60] for a review). Substantial F loss (30–50%) was only reported during major subaerial basaltic effusions [8,9]. We assess here that Etna basalt releases at most 15% of its fluorine during lateral dyke eruptions. A comparable estimate was derived from summit crater plume emissions [29], suggesting a similar behaviour of fluorine in the central volcano conduits. The shallower and more restricted exsolution of F than Cl during Etna basalt eruption is consistent with the ionic radius dependency of halogen partitioning between vapour and silicate melts [57,61].

5.2. Interpretation of measured Etna gas compositions

Our modelling can serve to interpret the compositional variations measured in Etna gas emissions. Here we illustrate this potential by looking at S/Cl and Cl/F ratios measured during three different types of activity in the period 2000–2002: (i) the 2002 lateral dyke eruption, (ii) the 14 June 2000 summit lava fountain and (iii) non-eruptive magma degassing across the summit craters. Most gas data were obtained using remote OP–FTIR spectroscopy [28,29,31,32] and, additionally, filter pack sampling [30].

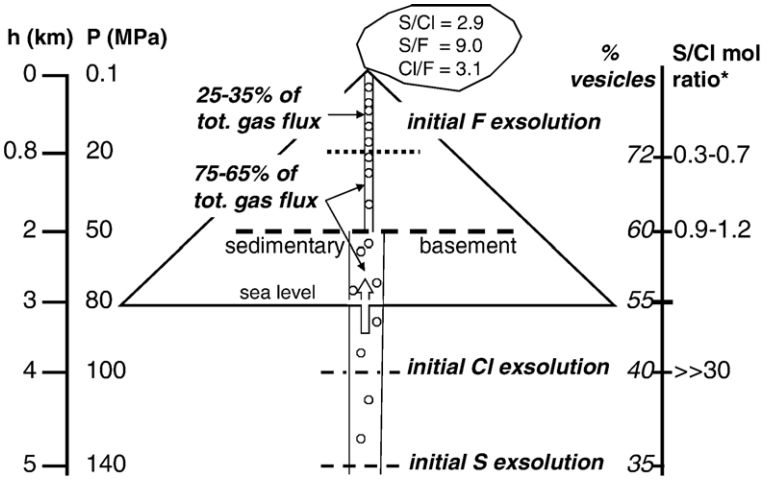

Fig. 7. Schematic drawing of Mount Etna volcanic conduits, lateral dykes and sub-volcanic plumbing system showing: (i) the initial pressures and depths of S, Cl and F exsolution with respect to the base of the pile and sea level; (2) the S/Cl ratio* of the gas phase that would exsolve from the magma in different depth intervals until the surface, without any deeper gas supply; and (3) the bulk vesicularity of magma rising in CSD conditions. The latter was computed from the cumulated amounts of H_2O and CO_2 exsolved between 400 MPa (1140 °C) – where the basaltic melt already coexists with 1.5 wt.% of gas – and 0.1 MPa (1100 °C). A mixed supply from shallow magma degassing in volcanic conduits and deeper-derived S-rich gas bubbles rising from below the volcanic pile is necessary to sustain the non-eruptive excess gas discharge with typical S/Cl (2.9), S/F (9) and Cl/F (3.1) molar ratios [29]. SO_2-rich gas bubbles derived from deeper than 0.8 km depth (20 MPa) in conduits supply 65–75% of the total gas output although they represent only 7% of total bubbles in volume. See text.

5.2.1. 2002 flank eruption

During this eruption an average S/Cl ratio of 5±1 was measured in the driving magmatic gases, except for a brief interval from 20 to 24 November 2002 in which the S/Cl ratio raised up to 19 before returning to its average value [29,32]. As shown by our modelling, a ratio of 5 is typical of closed system ascent of volatile-rich Etna basalt in a lateral dyke, with 35% average bulk Cl loss upon extrusion (Fig. 4a). Prevalent CSD conditions during this eruption are also supported by the evolution of dissolved H_2O and CO_2 in melt inclusions [12] and by the measured Cl/F and S/F ratios [29,30], that are close to our modelled ratios of 2 and 10 (Fig. 5a–b).

However, somewhat lower S/Cl values of ~3.5 were measured at the onset of the eruption (29 October 2002 [32]), during powerful fountaining of the most primitive magma (MgO ~ 7.5 wt.%). According to our model, they can be explained by enhanced chlorine release (55%) during more intense fragmentation of the magma, creating larger surfaces for Cl exchange between gas and melt and/or shortening the diffusion path of chlorine. Such an effect should be more pronounced in the external (more fragmented) envelop of a lava fountain – targeted in OP–FTIR measurements [31] – than in its inner part. In fact, we observed a minimal Cl loss (≤22%) in the matrix glasses and bulk samples of elongated, coarse scoria fragments that were most likely derived from the inner part of the fountains. Therefore, S/Cl ratios of ~3.5 recorded during most energetic fountaining in the 2002 but also 2001 [28] flank eruptions plausibly reflect enhanced fragmentation of magma erupting under CSD conditions.

Instead, the temporary increase of S/Cl ratio up to 19 on 24 November 2002 can only be explained by a transient opening of the system. This unique trend was associated with increasing SO_2 flux up to 28 000 t day^{-1} [32], but along with the extrusion of more evolved trachybasaltic magma (MgO ~ 5.5 wt.%; [12,32]). According to our model (Fig. 4a), the gradual S/Cl increase in that interval implies increasingly deeper bubble–melt separation in the erupting dyke, down to a depth of ~2 km below the vents (~50 MPa) on 24 November (Fig. 7). The mass of degassed melt required to supply the peaking SO_2 flux on that day can be assessed from the ratio ϕ_{SO_2}/X_{SO_2}, where X_{SO_2} is the weight fraction of SO_2 (~0.63 wt.%) released from the melt, given by melt inclusion data. We obtain 4.4×10^9 kg or, for a density of 2650 kg m^{-3}, a volume of 1.6×10^6 m^3 of melt. In our model, this melt rose under CSD conditions up to ~2 km below the vents, then its gas phase could separate and migrate differentially until eruptive release at the surface.

5.2.2. 14 June 2000 summit lava fountain

During this powerful lava fountain at the Southeast summit crater (SEC) OP–FTIR spectroscopic measurements revealed anomalously high S/Cl (10) and CO_2/S (10–8) molar ratios in the driving gas phase [31]. Based on melt inclusion data [13], these ratios were interpreted as reflecting the emptying of a bubble foam layer periodically accumulating on top of a magma body emplaced at ~1.5 km depth below SEC [31]. Our modelling allows refined assessment of this gas accumulation depth. Both trace element and melt inclusion data for the bulk rocks produced by periodical lava fountains at SEC in June 2000 [13,31] indicate that the supplied trachybasaltic magma was sulphide saturated and partially degassed (H_2O<2 wt.%; Fig. 6). Fig. 4b shows that, in such conditions, a S/Cl molar of 10 in the fountain gas implies a separate gas transfer from ~45 MPa or 1.8 km below the erupting crater.

5.2.3. Non-eruptive summit degassing

Besides eruptions, the prevalent manifestation of Etna is the voluminous plume gas release that persistently occurs from its summit craters, often without any lava extrusion. It was shown that this emission is sustained by underground degassing of about 4 times more magma than erupted on average [37], which implies extensive differential gas transfer (open system degassing) across the central conduits in non-eruptive periods. Melt inclusion data and our present modelling can provide further insight into the depth and the dynamics of the degassing processes at work.

The non-eruptive bulk plume emission displays variable S/Cl ratio in the range of 1.5–3.7 [29,38], with a mean of ~2.5±0.7. Note that such values are lower than the modelled bulk ratio (3.7) for closed system magma degassing in the central conduits, but also exclude a pure open degassing process – that would produce much lower ratios (Fig. 4b). We consider here a published set of representative S/Cl (2.9), S/F (9) and Cl/F (3.1) molar ratios that were remotely measured in early May 2001 using OP–FTIR spectroscopy [29]. These ratios constrain the respective contribution of each species to the total gas output, as:

$$\text{Total } F_{gas} = F_{SO_2} + F_{HCl} + F_{HF} = F_{SO_2}(1 + 1/R_{Cl} + 1/R_F) = 1.23F_{SO_2}$$

where R_{Cl} and R_F are the SO_2/HCl (5.15) and SO_2/HF (28.8) weight ratios of the volcanic plume. This

relationship holds whatever the absolute value of the total gas output. The pressures of initial exsolution of F and Cl provide vertical depth constraints on the magma volumes supplying the emitted F and Cl. In the central conduits of Etna all fluorine and most of chlorine are being outgassed between ~20 MPa (~800 m depth) and the surface. Data for melt inclusions and matrix glasses, corrected for differentiation, show that in this depth interval the magma releases 0.012 wt.% F, 0.065 wt.% Cl and either 0.019 wt.% S or 0.044 wt.% S depending on whether it is or not saturated with sulphide. The exsolving gas phase thus has HCl/HF, SO_2/HCl and SO_2/HF weight ratios of 2.9, 0.57 or 1.3, and 2.9 or 6.7, respectively, and its mass contribution to the total gas output is:

$$(F_{\text{gas}})_{<20\ \text{MPa}} = yF_{\text{SO}_2}(1 + 1/R_{\text{Cl}} + 1/R_{\text{F}})$$

While its HCl/HF ratio closely matches that of the volcanic plume, its SO_2/HCl and SO_2/HF ratios are ~4 to 10 times lower, implying that the proportion of the SO_2 flux arising from <20 MPa (y) ranges between ~25% and 10%. Depending on sulphide immiscibility, we thus find that between 65% and 75% of the total gas output, composed of 75–90% of total SO_2 and 7–10% of total chlorine, must originate from deeper than ~0.8 km below the air–magma interface (Fig. 7). This deeper-derived gas component is inferred to have a high S/Cl molar ratio of 29±2 and then to represent only ~7% in volume of the total gas sustaining the plume emission with S/Cl molar ratio of 2.9. Now, because it is responsible for 75% to 90% of the total SO_2 *mass* output, this implies that its carrying gas bubbles must be ≥10 times richer in sulphur on average than the bubbles formed at shallower (<20 MPa) depth.

What is the meaning of a bulk S/Cl ratio of 29±2 in this gas component coming from deeper than 20 MPa? Our modelling shows that such a ratio would be achieved at respective pressures of 65 and 80 MPa (depths of ~2.5 and 3.0 km) for closed system degassing of a magma unsaturated or saturated in sulphide (Fig. 4b). We emphasize here that the central conduits of Mount Etna are 2 to 2.5 km in height above the sedimentary basement of the volcanic pile (e.g. [62]) and that we inferred comparable depths of about 2 km for separate gas transfer responsible of S/Cl anomalies during the 2002 flank eruption (Section 5.2.1) and the 14 June 2000 lava fountain (Section 5.2.2). This suggests that favourable conditions (structural discontinuities, dyking, temporary magma ponding?) for bubble coalescence and differential gas transfer may exist at around the interface between the sedimentary basement and the volcanic pile. In addition, the high vesicularity of the magma at those depths (55% at 80 MPa and 60% at 50 MPa in CSD conditions, Fig. 7) could promote its permeability (e.g. [59,63–65]) and then separate gas flow [65]. Thus, one first interpretation of the S/Cl ratio of 29 in the deep gas component could be that magma initially rising in closed system in the sub-volcanic plumbing may start behave openly while reaching the bottom of narrower, 2–2.5 km high volcanic conduits, allowing its gas phase to migrate upward separately. Such an interpretation however requires that the uprising gas phase (i) would not re-equilibrate with bubbles formed at between ~2.5 km and 0.8 km in conduits and (ii) would rise fast enough to mix continuously and in steady proportion with shallower (<20 MPa) bubbles.

A simpler alternative interpretation would be that the S/Cl ratio of 29 integrates the contribution of bubbles formed at different depths in the volcanic and sub-volcanic plumbing system. We have shown that chlorine starts exsolving at ≤100 MPa or ~4 km depth below vents. Between that pressure and 20 MPa the magma can release a gas phase with S/Cl molar ratio of between 13 and 7 when it is unsaturated or saturated with sulphide. In that case, 55% to 75% of sulphur dioxide in the deep gas component should derive from ≥100 MPa. Given that sulphur starts to exsolve at ≤140 MPa, these SO_2-bearing bubbles could rise from 2 to 3 km depth below the base of the volcano (Fig. 7).

In order to maintain the non-eruptive excess gas discharge, differential gas transfer across the central conduits must be very efficient. Favourable conditions for that are (i) the high volatile content of Etna magma, (ii) its high vesicularity (Fig. 7) and (iii) slow magma rise in conduits (e.g. [66]). Here we assess the magma rise speed from the flux of HCl (~300 t day^{-1}) determined in early May 2001 [29] and the amount of chlorine degassed from the magma between 0.8 km depth and the surface. For a crystal content of 30%, we find that the daily HCl flux is supplied by the degassing of 1.6×10^5 m^3 of magma rising with a mean velocity of ~0.01 m s^{-1} in a conduit ~13 m in diameter. Such a velocity is indeed low enough to favour separate gas transfer. In order to maintain the mass fluxes and the chemical ratios of S, Cl and F at the surface, the ~800 m thick upper magma column, from which all fluorine and 93% of total chlorine are degassed, ought to be continuously renewed at an equivalent rate. Now, because the summit plume emission is supplied by the degassing of ~4 times more magma than erupted on average, convective drain back of the non-erupted degassed magma is also necessary [37]. In this mechanism, the surface gas output is limited by the rate at which gas-rich magma is supplied to the degassing cell and, in steady

state conditions, this latter should contain about as much degassed as undegassed magma [37,67]. The overall diameter of the conduit should then be twice the value computed above, i.e. about 26 m, which is of similar order as previously estimated from geophysical measurements [68]. In conclusion, both convective magma overturn and permeability-controlled degassing [65] plausibly act together to sustain the excess gas discharge of Etna.

6. Conclusions

The large data set available for CO_2, H_2O, S, Cl and F dissolved in olivine-hosted melt inclusions of Mount Etna lavas allows us to propose the first pressure-related modelling of S, Cl and F degassing during ascent, differentiation and eruption of water-rich basalt. The principal results are as follows:

(1) Sulphur, chlorine and fluorine display a contrasted outgassing behaviour during decompression of Etna basaltic magma. They start to exsolve at respective pressures of $\leq$140 MPa, $<$100 MPa and $\leq$10 MPa and are eventually degassed at >95%, 22–55%, and ~15% during eruptions. The variable degassing rate of chlorine is determined by the dynamics of magma ascent and extrusion.
(2) Fast ascent of the basaltic melt under closed system conditions results in 35% mean Cl loss and in bulk surface gas with S/Cl molar ratio of ~5.4, Cl/F ratio of 2 and S/F ratio of 10. This process accounts well for the time-averaged ratios measured during 2002-type lateral dyke eruptions. Greater magma fragmentation during powerful fountaining enhances Cl release and results in lower S/Cl ratio (3.7).
(3) Slower magma rise in larger central volcano conduits favours magma differentiation, sulphide immiscibility (temporarily depleting sulphur in the melt), and a more extensive degassing rate of chlorine (55%). This leads to a distinct evolution path of the gas phase. At between 30 and 50 MPa this latter has twice lower S/Cl ratio when the magma is sulphide saturated than when it is not, and the final S/Cl ratio in emitted gas depends on the degree of shallow aperture (open degassing) of the system.
(4) In both lateral dykes and central conduits, pre-eruptive separation of gas bubbles and differential gas transfer make S/Cl ratio increasing in surface gas. The high values (up to 19) measured during the 2002 eruption implies a transition from closed system to open system degassing, with separate gas transfer extending down to ~2 km below the vents (~50 MPa). Bubble–melt separation at a similar depth of (1.8 km) is inferred from the S/Cl ratio of 10 measured during summit fountaining of sulphide-saturated magma in June 2000 [31]. We outline that such a depth coincides with the base of the volcanic pile, where conditions favourable to gas accumulation and/or separate gas transfer may occur.
(5) Combining measurements of S/Cl/F ratios in gas emissions and petrological studies of co-erupted solid products provides strong insight into the mechanisms controlling lava fountains.
(6) Finally, the non-eruptive excess gas discharge from Mt. Etna summit craters requires differential transfer across the volcanic conduits of a mixed gas phase composed of (i) Cl–F-rich bubbles produced by shallow magma degassing in volcanic conduits and (ii) deeper-derived sulphur-richer bubbles originating from the sub-volcanic plumbing system. Both convective renewal of the volcanic conduits [37] and the high porosity–permeability of the magma [66] plausibly contribute to sustain this excess gas discharge.

Acknowledgments

We are particularly grateful to L. Raimbault (Ecole des Mines de Fontainebleau, France) for his help and participation to the fluorine data acquisition, to O. Belhadj for her help in sample preparation, and to our INGV colleagues in Catania for fruitful discussions. Thorough comments by two anonymous reviewers greatly helped us improving the quality of the manuscript.

References

[1] M.R. Carroll, J.D. Webster, Solubility of sulfur, noble gases, nitrogen, chlorine, and fluorine in magmas, in: M.R. Carroll, J.R. Holloway (Eds.), Volatiles in Magmas, vol. 30, Mineral. Soc. Amer., Washington, DC, 1994, pp. 231–279.
[2] A. Robock, C. Oppenheimer, Volcanism and the Earth's Atmosphere, AGU (Geophysical Monograph Series), vol. 139, 2003, p. 360.
[3] J.W. Hedenquist, J.B. Lowenstern, The role of magma in the formation of hydrothermal ore deposits, Nature 370 (1994) 519–527.
[4] I.A. Menyailov, Prediction of eruptions using changes in composition of volcanic gases, Bull. Volcanol. 39 (1975) 112–125.
[5] P. Allard, S. Alparone, M. Amore, N. Bruno, L. Brusca, M. Burton, T. Caltabiano, M. Mattia, F. Mure, E. Privitera, R. Romano, M. Rossi, T. Sgroi, L. Villari, Short-term variations in

magma dynamics at mount Etna detected by combined geochemical and geophysical monitoring (August–November 2000), European Geophys. Soc. Assembly, Nice, March 25–30 2001.
[6] A.T. Anderson, Chlorine, sulfur and water in magmas and oceans, Am. Bull. Geol. Soc. 85 (1974) 1485–1492.
[7] D.W. Muenow, D.G. Graham, N.W.K. Liu, J.R. Delaney, The abundance of volatiles in Hawaiian tholeiitic submarine basalts, Earth Planet. Sci. Lett. 42 (1979) 71–76.
[8] T. Thordarson, S. Self, Sulfur, chlorine and fluorine degassing and atmospheric loading by the Roza eruption, Columbia River Basalt Group, Washington, USA, J. Volcanol. Geotherm. Res. 74 (1996) 49–73.
[9] T. Thordarson, S. Self, N. Oskarsson, T. Hulsechosch, Sulfur, chlorine and fluorine degassing and atmospheric loading by the 1783–1784 AD (Skaftar Fires) eruption in Iceland, Bull. Volcanol. 58 (1996) 205–225.
[10] N. Métrich, A. Bertagnini, P. Landi, M. Rosi, Crystallization driven by decompression and water loss at Stromboli volcano (Aeolian Islands, Italy), J. Petrol. 42 (2001) 1471–1490.
[11] N. Métrich, P. Allard, N. Spilliaert, D. Andronico, M. Burton, 2001 flank eruption of the alkali- and volatile-rich primitive basalt responsible for Mount Etna's evolution in the last three decades, Earth Planet. Sci. Lett. 228 (2004) 1–17.
[12] N. Spilliaert, P. Allard, N. Métrich, A.V. Sobolev, Melt inclusion record of the conditions of ascent, degassing and extrusion of volatile-rich alkali basalt during the powerful 2002 flank eruption of Mount Etna (Italy), J. Geophys. Res. 111 (2006) B04203, doi:10.1029/2005/JB003934.
[13] N. Spilliaert, Dynamiques de remontée, dégazage et éruption des magmas basaltiques par les inclusions vitreuses et modelisation des processus dans le cas de l'Etna, 2000–2002, PhD Thesis IPG-Paris, 2006, pp 250.
[14] J.R. Delaney, D.W. Muenow, D.G. Graham, Abundance and distribution of water, carbon and sulfur in the glassy rims of submarine pillow basalts, Geochim. Cosmochim. Acta 42 (1978) 581–594.
[15] C.D. Byers, D.W. Muenow, M.O. Garcia, Volatiles in basalts and andesites from Galapagos spreading center, 85° to 86°, Geochim. Cosmochim. Acta 47 (1983) 1551–1558.
[16] P.J. Michael, J.G. Schilling, Chlorine in mid-ocean ridge magmas: evidence for assimilation of seawater-influenced components, Geochim. Cosmochim. Acta 53 (1989) 3131–3143.
[17] H. Bureau, N. Metrich, M. Semet, T. Staudacher, Fluid–magma decoupling in a hot spot volcano, Geophys. Res. Lett. 26 (1999) 3501–3504.
[18] J.E. Dixon, D.A Clague, P. Wallace, R. Poreda, Volatiles in alkali basalts from the North Arch Volcanic Field, Hawaii: extensive degassing of deep submarine-erupted alkalic series lavas, J. Petrol. 38 (1997) 911–939.
[19] C.K. Unni, J.G. Schilling, Cl and Br degassing by volcanism along the Reykjanes Ridge and Iceland, Nature 272 (1978) 19–23.
[20] T.M. Gerlach, Exsolution of H_2O, CO_2, and S during eruptive episodes at Kilauea volcano, Hawaii, J. Geophys. Res. 91 (12) (1986) 177–185.
[21] E.B. Watson, Diffusion in volatile-bearing magmas, in: M.R. Carroll, J.R. Holloway (Eds.), Volatiles in Magmas, vol. 30, Mineral. Soc. Amer., Washington, DC, 1994, pp. 371–409.
[22] P. Wallace, Volatiles in subduction zone magmas: concentrations and fluxes based on melt inclusion and volcanic gas data, J. Volcanol. Geotherm. Res. 140 (2005) 217–240.
[23] P. Allard, P. Jean-Baptiste, W. D'Alessandro, F. Parello, B. Parisi, C. Flehoc, Mantle-derived helium and carbon in groundwaters and gases of Mount Etna, Italy, Earth Planet. Sci. Lett. 148 (3–4) (1997) 501–516.
[24] N. Métrich, R. Clocchiatti, M. Mosbah, M. Chaussidon, The 1989–1990 activity of Etna magma mingling and ascent of H_2O–Cl–S-rich basaltic magma. Evidence from melt inclusions, J. Volcanol. Geotherm. Res. 59 (1993) 131–144.
[25] P. Allard, S. Alparone, D. Andronico, M. Burton, L. Lodato, F. Mure, T. Zgroi, Source process of cyclic fire fountaining at Mount Etna in 2000: a multidisciplinary study of the June 14 (63rd) event, Geophys. Res. Abstr. 5 (2003) 13079.
[26] S. La Delfa, G. Patane, R. Clocchiatti, J.-L. Joron, J.-C. Tanguy, The February 1999 fissure eruption of Mt Etna: inferred mechanism from seismological and geochemical data, J. Volcanol. Geotherm. Res. 105 (2001) 121–139.
[27] R. Moretti, Volatiles solubility with particular regard to sulphur species: theoretical aspects and application to Etnean volcanics, PhD Thesis, Univ. Pisa, Italy, 2001.
[28] P. Allard, A. Aiuppa, S. Bellomo, N. Bruno, M. Burton, T. Caltabiano, C. Federico, E. Longo, F. Mure, Evolution of magma degassing during the July–August 2001 eruption of Mount Etna tracked by COSPEC–FTIR remote sensing and filter pack sampling, Proceed. GNV Assembly, Roma, Italy, October 9–11 2001.
[29] M. Burton, P. Allard, F. Mure, C. Oppenheimer, FTIR remote sensing of fractional magma degassing at Mt. Etna, Sicily, Spec. Publ. - Geol. Soc. 213 (2003) 281–293.
[30] A. Aiuppa, C. Federico, G. Giudice, S. Gurrieri, A. Paonita, M. Valenza, Plume chemistry provides insights into mechanisms of sulfur and halogen degassing in basaltic volcanoes, Earth Planet. Sci. Lett. 222 (2004) 469–483.
[31] P. Allard, M. Burton, F. Mure, Spectroscopic evidence for a lava fountain driven by previously accumulated magmatic gas, Nature 433 (2005) 407–410.
[32] D. Andronico, et al., A multi-disciplinary study of the 2002–03 Etna eruption: insights into a complex plumbing system, Bull. Volcanol. 67 (2005) 314–330.
[33] P. Francis, A. Maciejewski, C. Chaffin, C. Oppenheimer, T. Caltabiano, SO_2 and HCl ratios in the plumes of Mount Etna and Vulcano determined by Fourier transform spectroscopy, Geophys. Res. Lett. 22 (1995) 1717–1720.
[34] M. Pennisi, M.-F. Le Cloarec, Variations of Cl, F, and S in Mount Etna's plume, Italy, between 1992 and 1995, J. Geophys. Res. 103 (B3) (1998) 5061.
[35] D.K. Chester, A.M. Duncan, J.E. Guest, C.R.J. Kilburn, Mount Etna: the Anatomy of a Volcano, Chapman and Hall, London, 1985 404 pp.
[36] S. Branca, P. Del Carlo, Eruption of Mt. Etna during the past 3200 years: a revised compilation integrating the historical and stratigraphic records, in: A. Bonaccorso, B. Calvari, M. Coltelli, C. Del Negro, S. Falsaperla (Eds.), Mt. Etna: Volcano Laboratory, Geophysical Monograph Series, vol. 143, AGU, Washington DC, 2004, pp. 49–64.
[37] P. Allard, Endogenous magma degassing and storage at Mount Etna, Geophys. Res. Lett. 24 (1997) 2219–2222.
[38] T. Caltabiano, M. Burton, S. Giammanco, P. Allard, N. Bruno, F. Mure, R. Romano, Volcanic gas emission from the summit craters and flanks of Mt. Etna, 1987–2000, in: A. Bonaccorso, B. Calvari, M. Coltelli, C. Del Negro, S. Falsaperla (Eds.), Mt. Etna: Volcano Laboratory, Geophysical Monograph Series, vol. 143, AGU, Washington DC, 2004, pp. 111–128.

[39] B. Bencke, M. Neri, The July–August 2001 eruption of Mt Etna (Sicily), Bull. Volcanol. 65 (2003) 461–476.
[40] R. Clocchiatti, M. Condomines, N. Guenot, J.-C. Tanguy, Magma changes at Mount Etna: the 2001 and 2002–2003 eruptions, Earth Planet. Sci. Lett. 226 (2004) 397–414.
[41] A. Bonaccorso, M. Aloisi, M. Mattia, Dike emplacement forerunning the Etna July 2001 eruption modelled through continuous tilt and GPS data, Geophys. Res. Lett. 29 (2002) 13.
[42] D. Patane, P. De Gori, C. Chiarabba, A. Bonaccorso, Magma ascent and the pressurization of Mount Etna's volcanic system, Science 299 (2003) 2061–2063.
[43] R.A. Corsaro, M. Pompilio, Dynamics of magmas at Mount Etna, in: A. Bonaccorso, B. Calvari, M. Coltelli, C. Del Negro, S. Falsaperla (Eds.), Mt. Etna: Volcano Laboratory, Geophysical Monograph Series, vol. 143, AGU, Washington DC, 2004, pp. 91–110.
[44] M. Mosbah, N. Métrich, P. Massiot, PIGME fluorine determination using a nuclear microprobe with application to glass inclusions, Nucl. Instrum. Methods Phys. Res., B 58 (1991) 227–231.
[45] S.M. Straub, G.D. Layne, The systematics of chlorine, fluorine and water in Izu arc front volcanic rocks: Implications for volatile recycling in subduction zones, Geochim. Cosmochim. Acta 67 (2003) 4179–4203.
[46] J.C. Tanguy, R. Clocchiatti, The Etnean lavas, 1977–1983: petrology and mineralogy, Bull. Volcanol. 47–4 (1984) 879–894.
[47] N. Metrich, R. Clocchiatti, Melt inclusion investigation of the volatile behavior in historic alkaline magmas of Etna, Bull. Volcanol. 51 (1989) 185–198.
[48] R. Clocchiatti, N. Metrich, Temoignages de la contamination dans les produits des eruptions explosives des Mts. Silvestri (1892) et Mts. Rossi (1669), Mt. Etna, Bull. Volcanol. 47/2 (1984) 909–928.
[49] S. Newman, J.B. Lowenstern, Volatilecalc: a silicate melt–H_2O–CO_2 solution model written in Visual Basic Excel, Comput. Geosci. 28 (5) (2002) 597–604.
[50] R.A. Corsaro, M. Pompilio, Buoyancy-controlled eruption of magmas at Mt Etna, Terra Nova 16 (1) (2004) 16–22.
[51] N. Métrich, P. Schiano, R. Clocchiatti, R. Maury, Transfer of sulfur in subduction settings: an example from Batan Island (Luzon volcanic arc, Philippines), Earth Planet. Sci. Lett. 167 (1999) 1–14.
[52] P. Allard, Geochimie isotopique et origine de l'eau, du carbone et du soufre dans les gaz volcaniques: Zones de rift, marges continentales et arcs insulaires, PhD Thesis, Paris 7 Univ. (1986) pp. 340.
[53] R. Moretti, P. Papale, On the oxidation state and volatile behavior in multi-component gas phase equilibria, Chem. Geol. 213 (1–3) (2004) 265–280.
[54] P.J. Jugo, R.W. Luth, J.P. Richards, Experimental data on the speciation of sulfur as a function of oxygen fugacity in basaltic melts, Geochim. Cosmochim. Acta 69 (2005) 497–503.
[55] N. Métrich, R. Clocchiatti, Sulfur abundance and its speciation in oxidized alkaline melts, Geochim. Cosmochim. Acta 60 (1996) 4151–4160.
[56] N. Métrich, M. Bonnin-Mosbah, J. Susini, B. Menez, L. Galoisy, Presence of sulphite (S^{IV}) in magmas: implications for volcanic sulphur emissions, Geophys. Res. Lett. 29/11 (2002) 33/1–33/4.
[57] J.G. Schilling, M.B. Bergeron, R. Evans, Halogens in the mantle beneath the North Atlantic, R. Soc. Phil. Trans., A 297 (1980) 147–178.
[58] T.M. Gerlach, E.J. Graeber, Volatile budget of Kilauea volcano, Nature 313 (1985) 273–277.
[59] J.E. Gardner, A. Burgisser, M. Hort, M. Rutherford, Experimental and model constraints on degassing of magma during ascent and eruption, in: C. Siebe, J.L Macias, G.J. Aguirre-Diaz (Eds.), Neogene–Quaternary Continental Margin Volcanism: A Perspective from Mexico: Geol. Soc. Amer. Spec. Paper 402, Penrose Conf. Series, 2006, pp. 99–113, doi:10.1130/2006.2402(04).
[60] A. Jambon, Earth degassing and large-scale geochemical cycling of volatile elements, in: M.R. Carroll, J.R. Holloway (Eds.), Volatiles in Magmas, vol. 30, Mineral. Soc. Amer., Washington, DC, 1994, pp. 479–509.
[61] H. Bureau, H. Keppler, N. Metrich, Volcanic degassing of bromine and iodine: experimental fluid/melt partitioning data and applications to stratospheric chemistry, Earth Planet. Sci. Lett. 183 (2000) 51–60.
[62] E. Lo Giudice, R. Rasa, Very shallow earthquake and brittle deformation in active volcanic areas: the Etnean region as an example, Tectonophysics 202 (1992) 257–268.
[63] C. Klug, K.V. Cashman, Permeability development in vesiculating-magmas: implications for fragmentation, Bull. Volcanol. 58 (1996) 87–100.
[64] J. Blower, Factors controlling permeability–porosity relationships in magma, Bull. Volcanol. 63 (2001) 497–504.
[65] M. Burton, H. Mader, M. Polacci, P. Allard, Constraints on the dynamics of degassing in basaltic systems, Eos, Trans. - AGU 86 (52) (2005) (Fall Meet. Suppl., Abstract V13G-01.
[66] R.S.J. Sparks, The dynamics of bubble formation and growth in magma: a review and analysis, J. Volcanol. Geotherm. Res. 3 (1978) 1–37.
[67] K. Kazahaya, H. Shinohara, G. Saito, Excessive degassing of Izu–Oshima volcano: magma convection in a conduit, Bull. Volcanol. 56 (1994) 207–216.
[68] H.J. Rymer, C.A. Locke, J.B. Murray, Magma movement in Etna volcano associated with the major 1991–1993 lava eruption: evidence from gravity and deformation, Bull. Volcanol. 57 (1995) 451–461.